A prognostic baseline blood biomarker and tumor growth kinetics integrated model in paclitaxel/platinum treated advanced non-small cell lung cancer patients

Francis Williams Ojara[1,2] | **Andrea Henrich**[1,2] | **Nicolas Frances**[3] | **Yomna M. Nassar**[1,2] | **Wilhelm Huisinga**[4] | **Niklas Hartung**[4] | **Kimberly Geiger**[5] | **Stefan Holdenrieder**[5] | **Markus Joerger**[6] | **Charlotte Kloft**[1]

[1]Department of Clinical Pharmacy and Biochemistry, Institute of Pharmacy, Freie Universitaet Berlin, Berlin, Germany

[2]Graduate Research Training Program PharMetrX, Berlin/Potsdam, Germany

[3]Department of Translational Modeling and Simulation, Roche Pharma Research and Early Development, Roche Innovation Center Basel, F. Hoffmann-La Roche Ltd, Basel, Switzerland

[4]Institute of Mathematics, University of Potsdam, Potsdam, Germany

[5]Munich Biomarker Research Center, Institute of Laboratory Medicine, German Heart Center, Technical University of Munich, Munich, Germany

[6]Department of Oncology and Hematology, Cantonal Hospital St. Gallen, St. Gallen, Switzerland

Correspondence

Charlotte Kloft, Department of Clinical Pharmacy and Biochemistry, Institute of Pharmacy, Freie Universitaet Berlin, Kelchstr. 31, Berlin 12169, Germany.
Email: charlotte.kloft@fu-berlin.de

Abstract

Paclitaxel/platinum chemotherapy, the backbone of standard first-line treatment of advanced non-small cell lung cancer (NSCLC), exhibits high interpatient variability in treatment response and high toxicity burden. Baseline blood biomarker concentrations and tumor size (sum of diameters) at week 8 relative to baseline (RS8) are widely investigated prognostic factors. However, joint analysis of data on demographic/clinical characteristics, blood biomarker levels, and chemotherapy exposure-driven early tumor response for improved prediction of overall survival (OS) is clinically not established. We developed a Weibull time-to-event model to predict OS, leveraging data from 365 patients receiving paclitaxel/platinum combination chemotherapy once every three weeks for ≤six cycles. A developed tumor growth inhibition model, combining linear tumor growth and first-order paclitaxel area under the concentration-time curve-induced tumor decay, was used to derive individual RS8. The median model-derived RS8 in all patients was a 20.0% tumor size reduction (range from −78% to +15%). Whereas baseline carcinoembryonic antigen, cytokeratin fragments, and thyroid stimulating hormone levels were not significantly associated with OS in a subset of 221 patients, and lactate dehydrogenase, interleukin-6 and neutrophil-to-lymphocyte ratio levels were significant only in univariate analyses (p value < 0.05); C-reactive protein (CRP) in combination with RS8 most significantly affected OS (p value < 0.01). Compared to the median population OS of 11.3 months, OS was 128% longer at the 5th percentile levels of both covariates and 60% shorter at their 95th percentiles levels. The combined paclitaxel exposure-driven RS8 and baseline blood CRP concentrations enables early individual prognostic predictions for different paclitaxel dosing regimens, forming the basis for treatment decision and optimizing paclitaxel/platinum-based advanced NSCLC chemotherapy.

Study Highlights

WHAT IS THE CURRENT KNOWLEDGE ON THE TOPIC?

Paclitaxel/platinum chemotherapy is the backbone of first-line treatment of advanced non-small cell lung cancer (NSCLC) albeit exhibiting high variability in treatment response and overall clinical outcomes. Although baseline blood biomarkers and early tumor response may support treatment monitoring and potentially guide treatment, quantitative models combining blood biomarkers and early tumor response are limited.

WHAT QUESTION DID THIS STUDY ADDRESS?

Does integrating data on baseline patient demographic/clinical characteristics, blood biomarker concentrations, and early tumor response, based on pharmacokinetic exposure-driven change in tumor size, improve the prediction of overall survival (OS) in patients with paclitaxel/platinum treated advanced NSCLC?

WHAT DOES THIS STUDY ADD TO OUR KNOWLEDGE?

Individual paclitaxel exposure-driven early tumor response combined with baseline blood biomarker concentrations in a prognostic model enhance prediction of OS for different paclitaxel dosing regimens: better week 8 tumor response and low baseline C-reactive protein concentrations predict significantly longer OS.

HOW MIGHT THIS CHANGE DRUG DISCOVERY, DEVELOPMENT, AND/OR THERAPEUTICS?

The developed prognostic model supports the improved identification of patients with advanced NSCLC receiving paclitaxel/platinum first-line chemotherapy with a poor clinical outcome.

INTRODUCTION

Lung cancer is the second most common malignancy and the leading cause of cancer-related deaths worldwide.[1] Non-small cell lung cancer (NSCLC) accounts for ~80% of all cases. Over 50% of patients with NSCLC initially present with metastatic disease (stage IV),[2,3] requiring systemic treatment.[2,3] Paclitaxel/platinum drug combinations are first-line treatment for advanced NSCLC.[4,5] This treatment is associated with variable response rates (35%–50%) and a high burden of dose-limiting toxicities, including myelosuppression and neuropathy.[6] Currently, there is no established prognostic factor for routine clinical use to predict poor treatment outcomes, ensure timely intervention, and circumvent needless toxicities.

Cancer-related blood biomarkers have been proposed for estimation of therapy response, prognosis, and early disease recurrence.[7,8] They offer a quick tissue noninvasive and cost-effective option for assessing health status and monitoring disease.[8,9] Carcinoembryonic antigen (CEA), soluble cytokeratin fragments (CYFRA 21-1), lactate dehydrogenase (LDH), interleukin-6 (IL-6), C-reactive protein (CRP), thyroid stimulating hormone (TSH), and neutrophil-to-lymphocyte ratio (NLR) are among other important blood biomarkers whose prognostic potential in NSCLC has been widely investigated[10–14] but not established in routine clinical use.

The predictive value of tumor response for overall survival (OS) has been documented for various cancers,[15–19] including paclitaxel/platinum-treated NSCLC.[17] To predict early response in solid tumors, parametric tumor growth inhibition (TGI) models describing tumor size across time have been developed from longitudinal tumor size data documented according to the Response Evaluation Criteria in Solid Tumors (RECIST).[20] These models often provide a more mechanistic description of the change in tumor size across time, accounting for the impact of treatment exposure or resistance development, and enable prediction of individual tumor response at specific timepoints.[21,22]

Parametric time-to-event (TTE) models are increasingly being exploited to characterize OS in oncology trials.[16,17,23] Parametric TTE models combining treatment exposure, early tumor response, patient characteristics, and broad blood biomarker panels have not been explored. Hence, the focus of this work was to (i) adequately characterize the change in tumor size across time for individual patients and identify the associated patient- and treatment-related factors, and (ii) jointly evaluate the prognostic value of baseline individual patient characteristics,

including blood biomarkers levels and the predicted early tumor response to chemotherapy, to improve the prediction of OS in patients with paclitaxel/platinum-treated advanced NSCLC and inform treatment to optimize chemotherapy.

METHODS

Demographic and clinical data

Data were obtained from the investigator-initiated CEPAC-TDM study, an open-label, randomized two-arm, phase III, multicenter study,[24] approved by the respective institutional review boards (Ostschweiz, St. Gallen in Switzerland and Eberhard-Karls-Universitaet, Tuebingen in Germany) and conducted according to the Declaration of Helsinki (ClinicalTrials.gov identifier NCT01326767). Briefly, 365 patients with newly diagnosed advanced NSCLC received paclitaxel (3-h intravenous infusion) plus carboplatin (target area under the plasma concentration-time curve [AUC] = 6 mg•min/ml) or cisplatin (80 mg/m^2) every three weeks for up to six cycles. In the body surface area (BSA)-guided dosing arm, 182 patients received standard paclitaxel doses of 200 mg/m^2 (734 cycles), whereas in the pharmacokinetic (PK)-guided dosing arm, 183 patients received PK-guided paclitaxel doses (720 cycles) according to an algorithm based on paclitaxel PK exposure and grade of neutropenia from the previous cycle.[24] PK sampling, for estimation of paclitaxel PK exposure, was performed only in the PK-guided dosing arm.[25] A summary of the dosing algorithm and patient characteristics were published before.[24]

Tumor size was evaluated in all patients using the RECIST criteria (version 1.1)[20] at baseline, day 1 of cycles 3 and 5, at the end of treatment visit (27–35 days after the last treatment dose), and during follow-up (every 3 months thereafter). The sum of diameters of the measured target lesions at each evaluation was calculated as tumor size.[20] Baseline (cycle 1, day 1) levels of blood biomarkers, CYFRA 21-1, CEA, LDH, CRP, IL-6, TSH, and NLR were measured in 221 patients. Biomarker analysis was performed at the Institute of Laboratory Medicine, Munich Biomarker Research Center, German Heart Center Munich, Technical University Munich/Germany, using standardized and quality-controlled processes (CRP: latex-enhanced turbidimetry on Cobas C501 analyzer; LDH: photometry on Cobas C501 analyzer; TSH, CEA, and CYFRA 21-1: electrochemiluminescence on Cobas E411 analyzer; all Roche diagnostics and IL-6: enzyme-linked immunosorbent assay on MesoScale SQ120). Patient OS was defined as the time between treatment initiation and patient death.

TGI model development based on PK-guided dosing arm data

Change in tumor size across time was described as a function of net tumor growth (during treatment because no longitudinal tumor size data was available before treatment) and drug-induced tumor decay[16] (Equation 1). Initially, only the PK-guided dosing arm data were used due to the availability of paclitaxel PK data. Data later than week 30 after treatment initiation were excluded to minimize the influence of post-study medication. Linear, exponential, and generalized logistic tumor growth models[22] were investigated. Drug-induced tumor decay was described as a first-order process with respect to tumor size (Equation 2) and linked to paclitaxel PK exposure (concentrations across time or AUC from start to end of a cycle based on a single paclitaxel dose administered on the first day of a 21-day cycle [AUC$_{cycle}$]) derived from a PK model developed from the PK-guided dosing arm data[25] (Equation 3). Joint evaluation of the impact of co-administered platinum drugs was not feasible due to parameter non-identifiability with paclitaxel and platinum drugs being administered in all patients at the same time. Furthermore, a decreasing drug effect over time was evaluated to account for resistance[16] (Equation 4).

$$\frac{dTS(t)}{dt} = k_{growth}(t) - k_{decay}(t) \qquad (1)$$

$$k_{decay}(t) = E_{drug}(t) \cdot TS(t) \qquad (2)$$

$$E_{drug}(t) = \beta(t) \cdot Exposure_{drug}(t) \qquad (3)$$

$$\beta(t) = \beta_0 \cdot e^{-\lambda \cdot t} \qquad (4)$$

in which $\frac{dTS(t)}{dt}$ denotes the time derivative of tumor size (TS); k_{growth} is the net tumor growth (linear, exponential, or logistic); k_{decay} is drug-induced decay; $\beta(t)$ is the drug-induced tumor decay rate constant per unit of paclitaxel exposure; β_0 is the drug-induced tumor decay rate constant per unit of paclitaxel exposure at time = 0; Exposure$_{drug}$ is paclitaxel concentration or AUC$_{cycle}$; λ is the rate constant for change in drug effect over time. Interindividual variability was estimated on the tumor growth and drug effect parameters using an exponential model.

The impact of baseline continuous covariates (number of lesions, tumor size, BSA, and age) and categorical baseline covariates (platinum drug: cisplatin vs. carboplatin; sex: male vs. female; tumor stage: IIIB vs. IV; tumor histology: non-squamous adenocarcinoma vs. squamous cell carcinoma; Eastern Cooperative Oncology Group [ECOG] performance status: 0/1 vs. 2) was evaluated against tumor growth and drug effect model parameters.

Linear, exponential, and power functions were evaluated for the continuous covariates whereas the proportional function was evaluated for the categorical covariates.

TGI model joint evaluation of BSA- and PK-guided dosing arms

To estimate parameters for the BSA- and PK-guided dosing arms combined, the multiple imputation approach[26–28] (Appendix S1; Figure S1) was applied based on the final TGI model from the PK-guided dosing arm. Individual paclitaxel PK exposure per cycle was derived across all patients by stochastic simulations (50 replicates) and used to estimate the TGI model parameters for all patients. Individual patient tumor size at week 8 relative to baseline was derived from the final parameters from the multiple imputation.

Impact of tumor size kinetics and baseline covariates on OS in BSA- and PK-guided dosing arms

To characterize the observed OS and evaluate the impact of patient characteristics and early tumor response on OS, the exponential and the Weibull parametric TTE models were evaluated. Only patients with baseline blood biomarker data for all the seven biomarkers ($n = 221$) were included to compare the impact of biomarkers on OS. Patient demographic/clinical characteristics were comparable between the two dosing arms (Table S1). The impact of age, sex, ECOG performance status, tumor stage, baseline tumor size, platinum drug type, prior adjuvant treatments, blood biomarkers levels, and week 8 relative to baseline (RS8) on OS was evaluated by stepwise covariate analysis[29]; a p value of <0.05 was used in the forward covariate inclusion step and <0.01 in the backward elimination step. The impact of identified covariates on OS was quantified by simulating clinical trials (250 replicates) at the 5th and 95th percentile of the continuous covariate distributions using the final covariate model and the distribution of the CEPAC-TDM dataset. For each simulation, Kaplan–Meier proportions of the surviving patients were computed across time for evaluation of median OS and the 90% confidence intervals around simulations were included based on the 5th and 95th percentiles of the estimated covariate effect parameters.

Model evaluation

Comparison of nested models used the likelihood ratio test with a decrease in the objective function value (OFV) ≥ 3.84 indicating statistical significance of the larger to the smaller model, given $\alpha = 0.05$ and one additional parameter. For non-nested models, the Akaike Information Criterion (AIC) with a drop in AIC of two was set as threshold for choosing the model with a lower AIC.[30] Additionally, precision of parameter estimates and simulation-based visual predictive checks (VPCs) were compared for different models.[31] Parametric TTE dropout modeling preceded creation of VPCs for the TGI models to account for patient dropout due to tumor progression (Appendix S1).

Software

Dataset preparation and statistical evaluation were performed in R (3.4.3).[32] TGI modeling was performed using the first-order conditional estimation method, whereas parametric TTE analysis was performed using the first-order method in NONMEM 7.3.0 which was sufficient because only one event was recorded per patient and no interindividual variability was estimated, with assistance of PsN (4.2.0)[33] and Pirana (2.9.4).[34]

RESULTS

Demographic and clinical data

Overall, in the 365 patients, 1353 tumor size observations were documented; 700 in the BSA-guided dosing arm and 653 in the PK-guided dosing arm. By week 30 after treatment initiation, 584 observations were recorded in the BSA-guided dosing arm and 572 in the PK-guided dosing arm. The average tumor size showed prominent early decline up to ~6 weeks after treatment initiation, gradually leveling-off followed by re-growth and was comparable between the two arms (Figure 1). A total of 84 patients had tumor assessment beyond week 30, with the remaining 281 dropping out due to tumor progression (48.8%), death (18.5%), adverse events (6.7%), or other reasons including withdrawal of consent (26.0%).

Baseline concentrations of all seven blood biomarkers were available in 221 patients (108 in BSA- and 113 in PK-guided dosing arms). Blood biomarker data were right-skewed (mean > median; Table S2). For these patients, by week 30 after treatment initiation, the BSA-guided dosing arm had 354 tumor size observations compared to 363 in the PK-guided dosing arm. A total of 70% ($n = 155$) of the patients had documented survival times whereas 66 patients were right-censored corresponding to the last recorded day in the study.
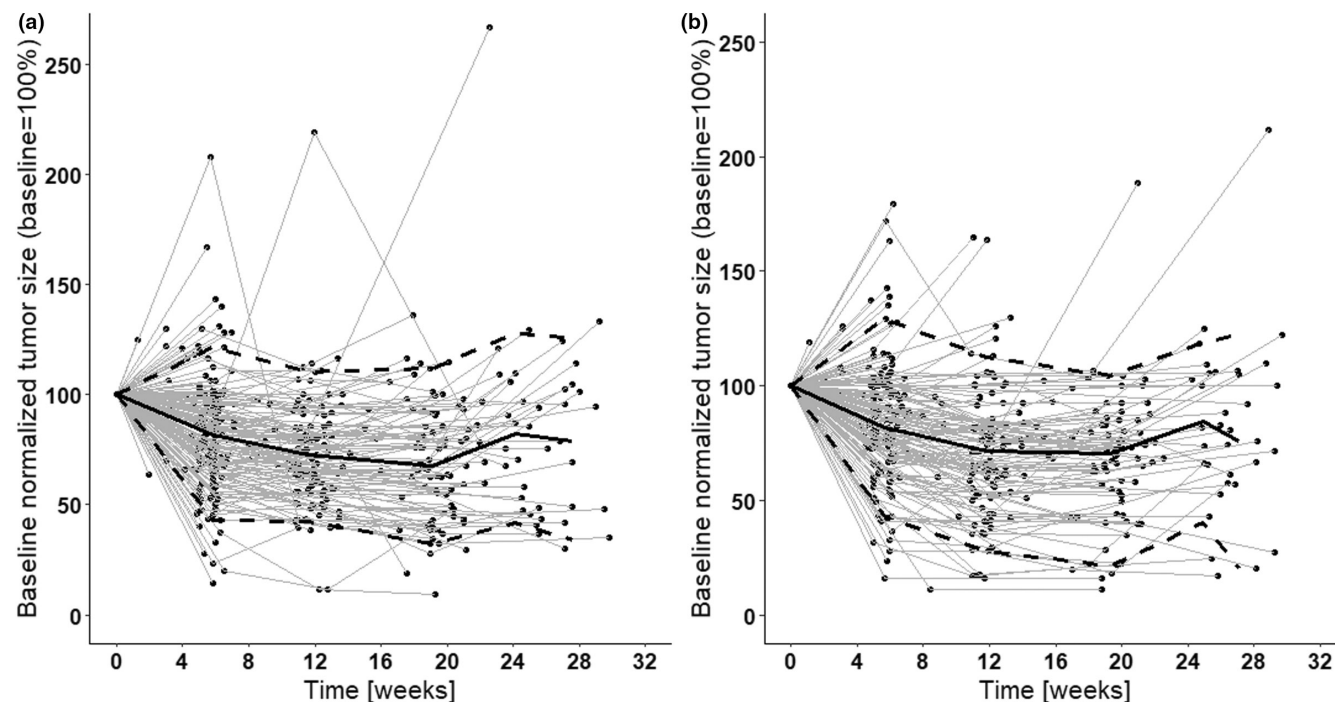
FIGURE 1 Individual tumor size across time normalized to baseline (=100%) up to week 30 after initiation of paclitaxel/platinum treatment in the two treatment arms. (a) Body surface area-guided dosing arm ($n = 700$ assessments from 182 patients). (b) Pharmacokinetic-guided dosing arm ($n = 653$ assessments from 183 patients). Points, tumor size data evaluated using the Response Evaluation Criteria in Solid Tumors (RECIST, version 1.1)[19]; black lines, median (solid), 5th and 95th percentiles (dashed) of observed tumor size data.

TGI model development based on PK-guided dosing arm data

A linear growth process, K_g, best characterized the net tumor growth regardless of whether paclitaxel concentrations or AUC_{cycle} was used as the driver of drug–induced tumor decay. Compared to the paclitaxel concentration-driven tumor decay (Table S3), paclitaxel AUC_{cycle}–driven tumor decay significantly improved model fit (ΔAIC of -29.5 points) and enabled estimation of a resistance term. High interindividual variability (coefficient of variation [CV] >70%) was estimated on tumor growth and drug-induced tumor decay parameters of both models. None of the covariates evaluated significantly impacted tumor growth kinetics, hence paclitaxel AUC_{cycle} was retained as the only driver of tumor size kinetics.

TGI model joint evaluation of BSA- and PK-guided dosing arms

TGI model parameters for BSA- and PK-guided dosing arms combined ($n = 365$ patients) were estimated by multiple imputation based on the paclitaxel AUC_{cycle}–driven tumor decay model (Table 1). Given the tumor

TABLE 1 Tumor growth inhibition model parameters with paclitaxel AUC_{cycle} as exposure metric in patients with advanced non-small cell lung cancer from the BSA- and PK-guided dosing arms combined.

Parameter (unit)	Parameter estimate (RSE, %)
Fixed-effect parameters	
K_g (µm/h)	1.03 (43.2)
β_{02_pac} (1/(µmol/L•h)/h)	$2.30 \cdot 10^{-5}$ (12.8)
λ (1/h)	$8.75 \cdot 10^{-4}$ (15.4)
Interindividual variability parameters	
K_g; CV, %	117 (41.3)
β_{01_pac}; CV, %	n.a.
β_{02_pac}; CV, %	86.3 (14.7)
λ; CV, %	53.9 (38.2)
Residual variability parameters	
Exponential model; CV, %	17.9 (7.17)

Abbreviations: AUC_{cycle}, paclitaxel area under the concentration-time curve from the start to end of a cycle; β_{02_pac}, paclitaxel AUC_{cycle}-driven tumor decay rate constant at start of treatment (time = 0); BSA, body surface area; CV, coefficient of variation; K_g, tumor growth rate constant for linear tumor growth; n.a., not applicable; PK, pharmacokinetic; RSE, relative standard error; λ, rate constant for exponential decline in drug effect over time.

growth rate constant (K_g) of 1.03 μm/h, the drug-induced tumor decay rate constant (β_{02_pac}) of $2.30 \cdot 10^{-5}$ (μmol/L·h)$^{-1} \cdot$h^{-1}, and a baseline tumor size of 8.3 cm (median in the CEPAC-TDM study), a paclitaxel AUC$_{cycle}$ threshold of 4.49 μmol·h/L (median AUC$_{cycle}$ [range] across cycles in all patients: 18.4 μmol·h/L [3.82–33.3]) was required to initiate tumor shrinkage at the beginning of treatment. The baseline drug effect (β_{02_pac}) exponentially declined at a rate, $\lambda = 8.75 \cdot 10^{-4} \cdot$h^{-1}, resulting in a 58.6% (46.1%–68.3%) reduction in drug effect on day 42 (end of cycle 2) and 82.9% (70.8%–90.0%) on day 84 (end of cycle 4; Figure S2).

Both paclitaxel concentration- and AUC$_{cycle}$–driven tumor decay models demonstrated similar predictive performances (Figure 2a,b, respectively), overpredicting higher tumor size observations. An exponential parametric TTE model was developed to characterize patient dropout across time. Higher tumor size at a specific time relative to baseline significantly increased the risk of patient dropout (Table S4, Figure S3). Accounting for patient dropout in the VPCs adjusted for the overpredictions of the higher tumor size observations (Figure 2b vs 2c), resulting in adequate prediction of general trends and variability in observed tumor size across time by the paclitaxel AUC$_{cycle}$–driven tumor decay model (Figure 2c: PK-guided dosing arm; 2d: all patients).

Based on different combinations of parameters of the paclitaxel AUC$_{cycle}$–driven TGI model, model-predicted tumor size trajectories of the median TGI parameter combination (50th percentiles for all model parameters), of "worst-case combination" (97.5th, 2.5th, and 50th percentiles for K_g, β_{02_pac}, and λ), and of "best-case combination" (2.5th, 97.5th, and 50th percentiles for K_g, β_{02_pac}, and λ) were generated: compared to the "median profile" (Figure 3a), the "worst-case combination" showed a more
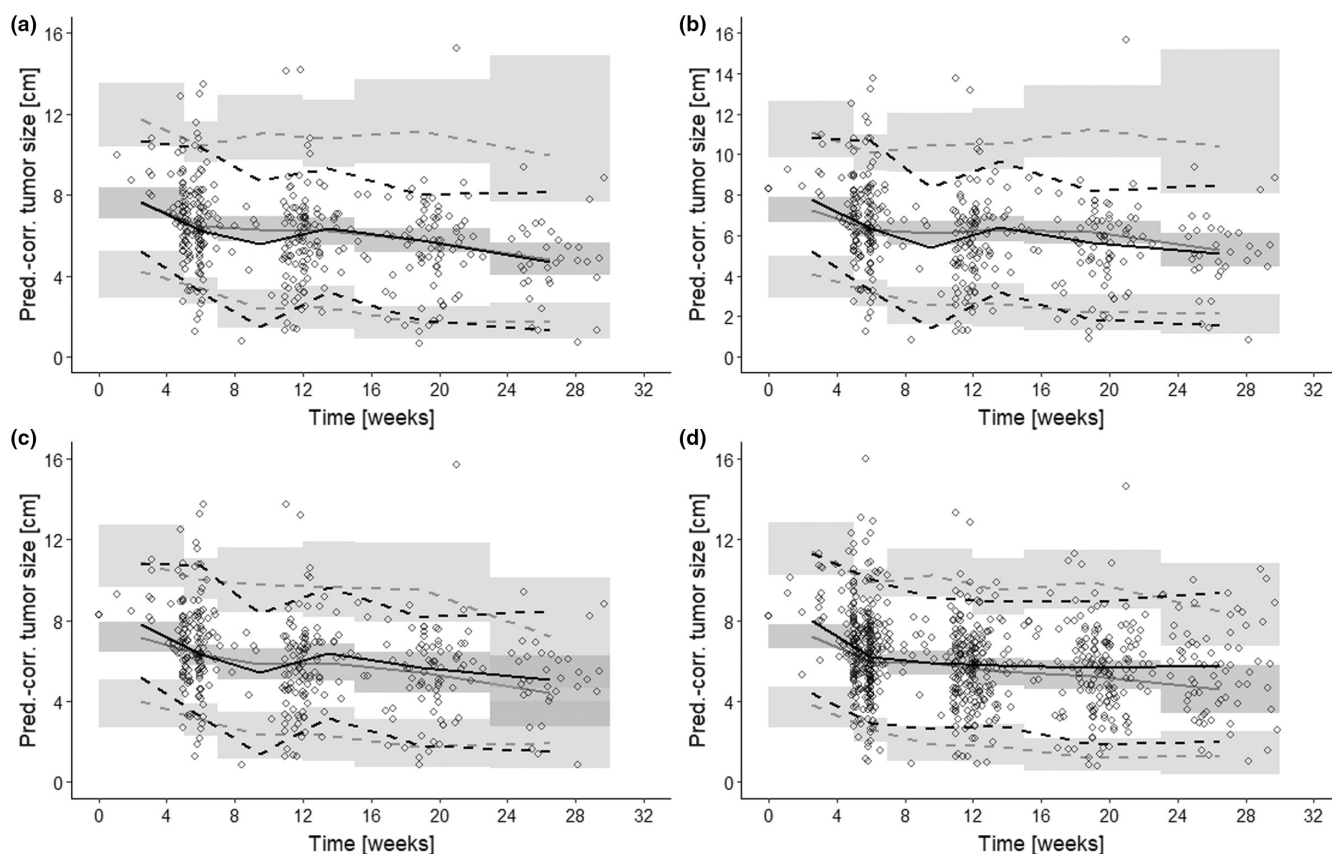

FIGURE 2 Prediction-corrected visual predictive checks for different tumor growth inhibition models. Black circles, observed tumor size (sum of diameters) data; black lines, median (solid), 5th and 95th percentiles (dashed) of observed tumor size data; gray lines, median (solid), 5th and 95th percentiles (dashed) of model-predicted tumor sizes; shaded areas, 90% confidence intervals of model-predicted percentiles. (a) Paclitaxel concentration-driven tumor decay not accounting for dropouts; (b) paclitaxel area under the concentration-time curve from start to end of a cycle (AUC$_{cycle}$)-driven tumor decay not accounting for dropouts; (c) paclitaxel AUC$_{cycle}$-driven tumor decay accounting for dropout; and (d) paclitaxel AUC$_{cycle}$-driven tumor decay based on imputed paclitaxel AUC$_{cycle}$ and accounting for dropouts. Panels a to c were derived from the pharmacokinetic (PK)-guided dosing arm data whereas d was derived from both the body surface area- and pharmacokinetic-guided dosing arm data combined. For panels b to d, a parametric time-to-event dropout model, describing the change in tumor size at a specific timepoint relative to baseline, as a key predictor of dropout, was developed based on the observed patient dropout data and used in simulations for the visual predictive checks.
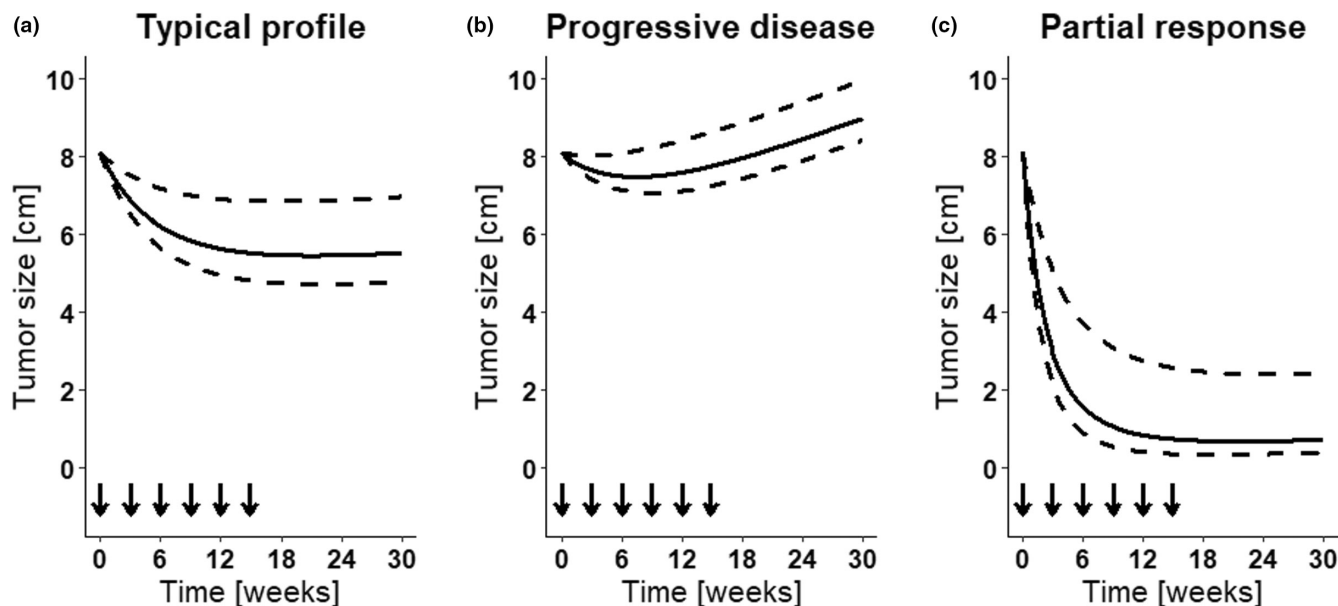
FIGURE 3 Tumor size (sum of diameters) across time from simulations using different combinations of tumor growth and drug effect parameters estimated from the tumor growth inhibition (TGI) model with paclitaxel area under the concentration-time curve from start to end of a cycle (AUC_{cycle})-driven tumor decay assuming the median baseline tumor size in the CEPAC-TDM study (8.3 cm). Lines, median (solid), 5th and 95th percentiles (dashed) of tumor size across time based on the distribution of paclitaxel AUC_{cycle}; vertical arrows, time points of paclitaxel administration at the cycle start. Panels show profiles for different combinations of estimated tumor growth rate constant (K_g) and paclitaxel AUC_{cycle}-driven tumor decay rate constant (β_{02_pac}). (a) Median TGI model parameter combination (50th percentiles for all model parameters); (b) "worst case combination" parameters (97.5th, 2.5th, and 50th percentiles for K_g, β_{02_pac}, and λ); (c) "best-case combination" parameters (2.5th, 97.5th, and 50th percentiles for K_g, β_{02_pac}, and λ). Compared to the "median profile" (panel a) the "worst combination case" showed a much more pronounced tumor size increase over time comparable to a "progressive disease" cohort (panel b) and the "best case combination" case a continuous decease in tumor size over time comparable to a "partial/complete response" cohort (panel c).

pronounced tumor size increase over time comparable to a "progressive disease" (Figure 3b) and the "best-case combination" showed a continuous decrease in tumor size over time comparable to "partial/complete response" (Figure 3c). The median model-derived tumor size at RS8 across all evaluated patients corresponded to a 20% reduction (range from −78% to +15%).

Impact of tumor size kinetics and baseline covariates on OS in BSA- and PK-guided dosing arms

OS was better described by the Weibull model, compared to the exponential parametric TTE model, with a 5.06-point drop in OFV (1 additional parameter, Table 2, left and middle columns). The instantaneous risk of death (hazard, $h(t)$, per hour) for the Weibull model was computed from the hazard scale factor (λ_{OS}) and hazard shape factor (α). The instantaneous risk per 10,000 patients increased with time, initially 4 (week 1), 5 (end of cycle 1), and 10 (at 6 months). This model adequately predicted

TABLE 2 Parameters from time-to-event analysis of overall survival (3 models) in patients with advanced non-small cell lung cancer with baseline measurements of all seven blood biomarkers.

Parameter (unit)	Parameter estimate (RSE, %)		
	Exponential parametric TTE base model	Weibull parametric TTE base model	Weibull parametric TTE covariate model
Fixed-effects parameters			
λ_{OS_0} (1/h)	0.000090 (7.60)	n.a.	n.a.
λ_{OS} (1/h)	n.a.	0.000090 (7.00)	0.00010 (7.30)
α	n.a.	1.17 (6.70)	1.29 (6.90)
Covariate effect parameters			
CRP on λ	n.a.	n.a.	0.00744 (16.9)
RS8 on λ	n.a.	n.a.	0.0233 (26.6)

Abbreviations: λ_{OS_0}, constant baseline hazard of the exponential parametric time-to-event (TTE) model; λ_{OS}, hazard scale factor for the Weibull parametric TTE model; CRP, C-reactive protein concentration at baseline; n.a., not applicable; RS8, tumor size at week 8 relative to baseline; RSE, relative standard error; α, shape factor of the Weibull parametric TTE model.
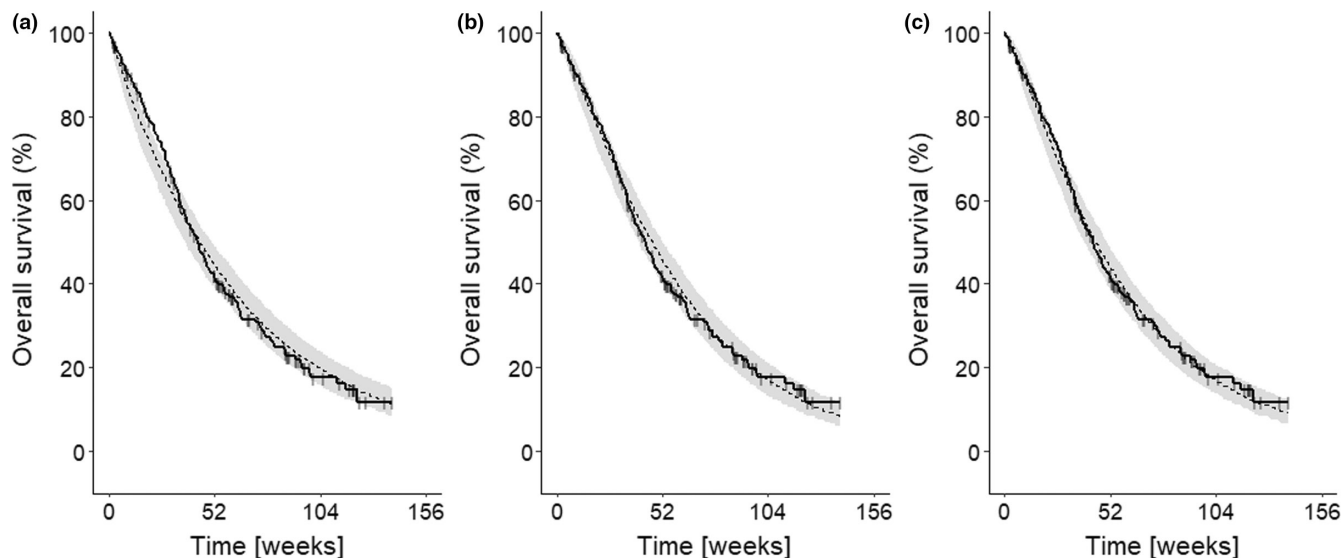
FIGURE 4 Kaplan–Meier visual predictive checks comparing predictive performance of different parametric time-to-event (TTE) models to the observed overall survival data in patients with baseline measurements for all seven blood biomarkers (n = 221) from the CEPAC-TDM trial. Solid line, observed survival data (vertical lines represent censoring times corresponding to the time of patients' last participation in the study); dashed line, median model-predicted profile, with 90% confidence interval (gray shade). (a) Exponential parametric TTE base model with no covariates; (b) Weibull parametric TTE base model with no covariates; (c) Weibull parametric TTE covariate model including baseline C-reactive protein concentrations and tumor size at week 8 relative to baseline as covariates predictive of overall survival.

the OS, whereas the exponential model overpredicted the hazard at times <40 weeks (Figure 4a,b) and was adopted as the base model.

Baseline CRP concentration and RS8 significantly affected OS (p value <0.01) in the final covariate model (Equation 5, Table 2, right column) after stepwise covariate modeling, with a 43.0-point drop in OFV compared to the base model (2 additional parameters).

$$h(t) = \lambda_{OS} \cdot \alpha \cdot (\lambda_{OS} \cdot t)^{\alpha-1} \cdot \exp\left(E_{RS8} \cdot (RS8 - RS8_{med})\right) \\ \cdot \exp\left(E_{CRP} \cdot (CRP - CRP_{med})\right) \quad (5)$$

where $h(t)$ is the hazard of death, λ_{OS} is the hazard scale factor, α is the hazard shape factor, E_{RS8} and E_{CRP} are covariate effect parameters quantifying the change in $h(t)$ per unit change in RS8 and CRP relative to their median values (i.e., $RS8_{med}$ and CRP_{med}, respectively).

The Weibull parametric TTE covariate model adequately predicted the general trends of observed OS in the entire population (Figure 4c; NONMEM code, Appendix S1), generally capturing profiles of different patient cohorts categorized based on the median (above/median) of investigated covariates (Figure S4). Baseline LDH activity, IL-6 concentration, baseline tumor size, and NLR only significantly impacted OS in univariate analysis (p value <0.05) whereas all other evaluated covariates, excluding baseline CRP concentration and RS8, did not significantly impact OS. A significantly longer OS was predicted at low baseline CRP and low RS8 (Figure 5). Compared to the typical median value of 45 weeks, the OS was +82.2% for a relative tumor size reduction of 57.6% (5th percentile RS8) and −24.4% for a tumor size reduction of 8.60% (95th percentile). Likewise, OS was +26.7% for a baseline CRP of 1.18 mg/L (5th percentile) and −46.7% for a baseline CRP of 151 mg/L (95th percentile; Table S5). Figure 5 depicts the simulated time-course of OS for the 5th and 95th percentiles of CRP and RS8, respectively. Patients with the 5th percentile covariate levels for both RS8 and baseline CRP concentrations had a +128% OS (i.e., 103 weeks) compared to the median OS (45 weeks), in contrast to the −60% OS (i.e., 18.2 weeks) for patients with the 95th percentile covariate levels.

DISCUSSION

We successfully developed a parametric TTE model combining individual patient baseline serum CRP concentrations and early tumor response to improve the prediction of OS in patients with paclitaxel/platinum treated advanced NSCLC: low inflammation (low baseline CRP concentrations) at treatment start and better early tumor response (i.e., lower tumor size at RS8) predicted favorable OS: a CRP concentration of 1.2 mg/L plus a 58% tumor size reduction at week 8 were associated with approximately twofold longer OS. This model enables early individual prognostic prediction and could facilitate early
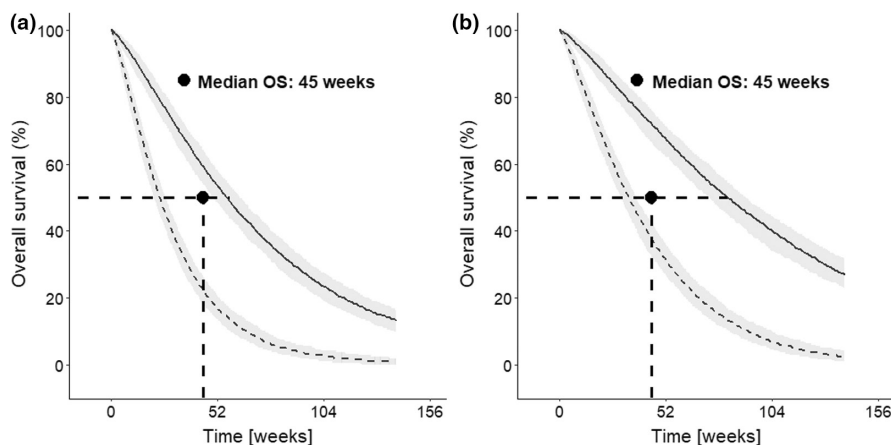
FIGURE 5 Predicted time profiles for overall survival (OS) for the 5th and 95th percentile covariate levels of baseline C-reactive proteins (CRP; panel a) and tumor size at week 8 relative to baseline (RS8, panel b) in patients with baseline measurements for all seven biomarkers ($n = 221$) from the CEPAC-TDM trial based on the Weibull parametric time-to-event covariate model. Solid lines, 5th percentile covariate level (RS8 = 42.4%, CRP = 1.18 mg/L); dashed lines, 95th percentile covariate level (RS8 = 91.4%, CRP = 151 mg/L); shaded areas, 90% confidence intervals.

assessment of treatment benefit/non-benefit for therapy decisions, to optimize paclitaxel/platinum-based advanced NSCLC chemotherapy.

Empirical parametric TGI models are valuable for characterizing tumor size kinetics from sparse tumor size data in oncology trials.[17,21] A constant linear tumor growth and a first-order paclitaxel-induced tumor decay best characterized the tumor size kinetics in this study, consistent with previous findings in patients with paclitaxel/carboplatin-treated NSCLC,[17] and in necitumumab/gemcitabine/cisplatin-treated patients.[15] Unlike the previous study,[17] within which drug-induced tumor decay was not linked to treatment exposure, we characterized drug-induced tumor decay as a function of paclitaxel PK exposure. This enabled characterization of the impact of changing drug exposure across cycles on tumor growth kinetics (e.g., due to the often unavoidable dose adaptations in the clinical setting). This further facilitated simulation-based exploration of tumor growth kinetics with different paclitaxel exposure levels (Figure 3) or derivation of tumor growth kinetics for patients treated with different paclitaxel dosing regimens.

To describe tumor size profiles in all patients, while accounting for missing paclitaxel PK data in the BSA-guided dosing arm, the multiple imputation approach[26–28] was used, accounting for the impact of variability in paclitaxel PK on the TGI model parameters for realistic characterization of the individual tumor size profiles. The decline in drug effect across time may be attributed to development of resistance to the administered chemotherapy drugs.[35] Given a baseline tumor size of 8.3 cm and paclitaxel AUC_{cycle} of 18.3 µmol·h/L (medians in the CEPAC-TDM study), the estimated

tumor decay rate constant (β_{02_pac}) of $2.30 \cdot 10^{-5}$ (µmol/L·h)$^{-1}$·h^{-1} translates into an initial tumor shrinkage rate of 0.587 cm/week, comparing well with the 0.304 cm/week derived from earlier findings in patients with paclitaxel/carboplatin-treated NSCLC.[17] Across all patients, a median 20% reduction (range from −78% to +15%) of tumor size relative to baseline was estimated after 2 months, consistent with the diverse RECIST tumor size profiles observed after 2 months in patients with advanced NSCLC treated with paclitaxel/platinum-containing chemotherapy, predominantly reporting stable disease but also partial response and progressive disease.[36,37]

The risk of patient death (OS) increased with time after treatment initiation. A better early tumor response improved OS. The 5th and 95th percentiles of RS8 were associated with 82.2% longer OS and 24% shorter OS, respectively, compared to the median of 45 weeks. The link between lower RS8 and improved OS has been previously reported in patients with advanced NSCLC receiving diverse chemotherapy options,[17] including paclitaxel/carboplatin. These findings are consistent with the inverse relation showing the longest OS with the smallest tumor growth rate constant (corresponding to lower RS8) in atezolizumab-treated solid tumors.[23] RS8 better predicted OS compared to week 4 or 6 tumor response,[17] hence was adopted in this work. For patients surviving <8 weeks, week 8 tumor size was predicted using the TGI model for OS evaluation. Combining early tumor response with patient characteristics, such as ECOG status, has been shown to improve the prediction of OS from parametric TTE analysis across different tumor entities.[17,18,38] Our stringent stepwise statistical covariate evaluation revealed

a combination of RS8 and baseline serum CRP concentration as most predictive of OS. The 5th and 95th percentiles of baseline serum CRP were associated with a +26.7% OS and a −46.7% OS, respectively, compared to the typical median value of 45 weeks.

Our finding relating low baseline serum CRP concentrations with longer OS is consistent with previous works.[10–12] CRP is a hepatocellular acute-phase-protein whose serum concentration dramatically rises during inflammation or infection.[39] Chronic systemic inflammation in advanced NSCLC results from tumor necrosis or local tissue damage resulting into elevation of serum CRP concentrations.[40,41] CRP synthesis is mediated by IL-6, a pro-inflammatory cytokine synthesized by various inflammatory cells.[42] The molecular link between serum CRP and NSCLC treatment outcome is not fully clear; however IL-6, a mediator of cancer resistance, seems to be involved. IL-6 synthesis was upregulated in paclitaxel-treated ovarian cancer cells and platinum-induced IL-6 expression in brain cancer increased the tumorigenic potential.[12] Hence IL-6-mediated tumorigenic effects, coupled with IL-6-mediated CRP synthesis may explain the relationship between CRP and OS. High baseline blood IL-6, LDH, and NLR predicted a shorter OS only in univariate analysis (p value <0.05). CRP, IL-6, LDH, and NLR are all nonspecific markers of systemic inflammation and elevated levels have been linked to poor prognosis in several cancers.[43] High baseline serum CYFRA 21-1 and CEA levels, the two evaluated tumor markers, were not significantly associated with OS, contrary to earlier reports.[44] Additionally, high baseline circulating TSH did not significantly increase OS, contrary to earlier reports.[14]

To the best of our knowledge, this work represents the first broad evaluation incorporating (a) early tumor response, based on individual drug exposure and tumor size, and (b) baseline patient characteristics including a broad panel of blood biomarkers. Chan et al.[23] recently evaluated tumor response, baseline patient characteristics including blood biomarkers (CRP, LDH, albumin and NLR) on survival, and Gavrillov et al.[45] evaluated tumor size and NLR. In both cases, tumor size dynamics was not linked to treatment exposure.[23] This pharmacometric model-based integration of knowledge from diverse sources represents a more efficient use of clinical trial data and hence more apt to maximize efficacy and/or reduce treatment-related toxicity, and is in line with the principles of Model-Informed Precision Dosing for treatment optimization.[46–48] Advanced diagnostic and bioanalytical techniques enable quantification of patient variables of the parametric TTE model of OS. Tumor size is typically measured noninvasively using imaging techniques, such as X-ray or computed tomography scans, whereas a validated method applicable for routine clinical quantification of paclitaxel plasma concentrations,[49] and established point of care methods for evaluating CRP concentrations have been developed.[50] Given that CRP measurements are method dependent, re-evaluation of the model is required in case a different analyzer is used. Individual patient OS predicted using the developed model can be combined with other patient characteristics, such as performance status or occurrence of adverse effects for therapeutic decision making.

As for the limitations, first, this analysis only accounted for the impact of paclitaxel PK exposure on tumor growth kinetics and not the co-administered platinum drugs due to parameter nonidentifiability. Additionally, the impact of second-line treatments administered after the paclitaxel/platinum was not accounted for. Hence, the strength of paclitaxel-induced drug effect might be inflated. However, dose adaptations across cycles were more prominent for paclitaxel compared to the platinum drugs,[24] therefore accounting for paclitaxel PK exposure alone still reflects the impact of changing chemotherapy drug exposure of tumor growth kinetics. Second, the number of patients included in the current evaluation is lower than in previous evaluations,[17,23] with a possible implication on covariate selection in the final model. However, our informative dataset with patient demographics, in particular PK exposure, tumor size and OS, enabled establishment of this robust prognostic evaluation framework, which should be tested on a larger sample size. Third, the impact of blood biomarkers was evaluated only at baseline making it impossible to account for the impact of treatment on biomarker concentrations. Because biomarker sampling frequencies varied across time in the 221 patients, their impact on OS could only be compared across the seven biomarkers at baseline. Nevertheless, their impact over time should be assessed in the future.

In conclusion, we developed a parametric TTE model combining individual patient baseline serum CRP concentrations and exposure-driven early tumor response as the most significant predictors of OS after evaluating several patient characteristics including baseline levels of seven blood biomarkers (CRP, IL-6, CEA, TSH, CYFRA 21-1, LDH, and NLR). High baseline serum CRP concentration and poor early tumor response predicted a shorter OS. This parametric TTE model supports identification of patients with advanced NSCLC receiving paclitaxel/platinum first-line chemotherapy with a poor clinical outcome for therapeutic decision making to contribute to the optimization of their paclitaxel/platinum chemotherapy.

AUTHOR CONTRIBUTIONS

F.W.O. wrote the first draft of the manuscript. F.W.O., A.H., N.F., W.H., N.H., K.K., S.H., M.J., and C.K. designed the research. F.W.O., A.H., N.F., Y.M.N., W.H., N.H.,

K.K., S.H., M.J., and C.K. performed the research. F.W.O., A.H., and Y.M.N. analyzed the data. All authors read and approved the submission of this manuscript to *CPT: Pharmacometrics and Systems Pharmacology*.

CONFLICT OF INTEREST STATEMENT
C.K. and W.H. report grants from an industry consortium (AbbVie Deutschland GmbH & Co. K.G., Astra Zeneca, Boehringer Ingelheim Pharma GmbH & Co. K.G., Grünenthal GmbH, F. Hoffmann-La Roche Ltd, Merck KGaA, Sanofi and Novo Nordisk) for the PharMetrX program. C.K. reports grants from the Innovative Medicines Initiative-Joint Undertaking ("DDMore") and the Federal Ministry of Education and Research within the Joint Programming Initiative on Antimicrobial Resistance (JPIAMR), all outside the submitted work. M.J reports advisory roles (institutional): Novartis, Astra Zeneca, Basilea Pharmaceutica, Bayer, BMS, Debiopharm, MSD, Roche, Sanofi; research funding: Swiss Cancer Research; travel grants: Roche, Sanofi, Takeda. All other authors declared no competing interests for this work.

ORCID
Andrea Henrich https://orcid.org/0000-0003-0072-8352
Yomna M. Nassar https://orcid.org/0000-0003-0507-7130
Wilhelm Huisinga https://orcid.org/0000-0002-5249-3914
Niklas Hartung https://orcid.org/0000-0002-4000-6525

REFERENCES
1. Sung H, Ferlay J, Siegel RL, et al. Global cancer statistics 2020: GLOBOCAN estimates of incidence and mortality worldwide for 36 cancers in 185 countries. *CA Cancer J Clin*. 2021;71:209-249.
2. Molina JR, Yang P, Cassivi SD, Schild SE, Adjei AA. Non-small cell lung cancer: epidemiological, risk factors, treatment, and survivorship. *Mayo Clin Proc*. 2008;83:584-594.
3. Duma N, Santana-Davila R, Molina JR. Non–small cell lung cancer: epidemiology, screening, diagnosis, and treatment. *Mayo Clin Proc*. 2019;94:1623-1640.
4. Novello S, Barlesi F, Califano R, et al. Metastatic non-small-cell lung cancer: ESMO clinical practice guidelines for diagnosis, treatment and follow-up. *Ann Oncol*. 2016;27:V1-V27.
5. Planchard D et al. Metastatic non-small cell lung cancer: ESMO clinical practice guidelines for diagnosis, treatment and follow-up. *Ann Oncol*. 2018;29:iv192-iv237.
6. Ramalingam S, Belani CP. Paclitaxel for non-small cell lung cancer. *Expert Opin Pharmacother*. 2004;5:1771-1780.
7. Holdenrieder S, Stieber P. New challenges for laboratory diagnostics in non-small cell lung cancer. *Cancer Biomark*. 2009;6:119-121.
8. Holdenrieder S. Biomarkers along the continuum of care in lung cancer. *Scand J Clin Lab Invest Suppl*. 2016;245:S40-S45.
9. Nakamura H, Nishimura T. History, molecular features, and clinical importance of conventional serum biomarkers in lung cancer. *Surg Today*. 2017;47:1037-1059.
10. Ni XF, Wu P, Wu CP, et al. Elevated serum C-reactive protein, carcinoembryonic antigen and N2 disease are poor prognostic indicators in non-small cell lung cancer. *Asia Pac J Clin Oncol*. 2015;11:e22-e30.
11. Fiala O, Pesek M, Finek J, et al. Prognostic significance of serum tumour markers in patients with advanced-stage NSCLC treated with pemetrexed-based chemotherapy. *Anticancer Res*. 2016;36:461-466.
12. Xiao X. C-reactive protein is a significant predictor of improved survival in patients with advanced non-small cell lung cancer. *Medicine*. 2019;98:e16238.
13. Silva EM, Mariano VS, Pastrez PRA, et al. High systemic IL-6 is associated with worse prognosis in patients with non-small cell lung cancer. *PLoS One*. 2017;12:e0181125.
14. Degirmencioglu S et al. Effects of serum thyroid stimulating hormone levels on prognosis in patients with advanced non-small cell lung cancer. *J Carcinog Mutagen*. 2016;7:1000272.
15. Chigutsa E, Long AJ, Wallin JE. Exposure-response analysis of necitumumab efficacy in squamous non-small cell lung cancer patients. *CPT Pharmacometrics Syst Pharmacol*. 2017;6:560-568.
16. Claret L, Girard P, Hoff PM, et al. Model-based prediction of phase III overall survival in colorectal cancer on the basis of phase II tumor dynamics. *J Clin Oncol*. 2009;27:4103-4108.
17. Wang Y, Sung C, Dartois C, et al. Elucidation of relationship between tumor size and survival in non-small-cell lung cancer patients can aid early decision making in clinical drug development. *Clin Pharmacol Ther*. 2009;86:167-174.
18. Feng Y, Wang X, Suryawanshi S, et al. Linking tumor growth dynamics to survival in ipilimumab-treated patients with advanced melanoma using mixture tumor growth dynamic modeling. *CPT Pharmacometrics Syst Pharmacol*. 2019;8:825-834.
19. Bruno R, Bottino D, de Alwis DP, et al. Progress and opportunities to advance clinical cancer therapeutics using tumour dynamic models. *Clin Cancer Res*. 2020;26:1787-1795.
20. Eisenhauer EA, Therasse P, Bogaerts J, et al. New response evaluation criteria in solid tumours: revised RECIST guideline (version 1.1). *Eur J Cancer*. 2009;45:228-247.
21. Park K. A review of modeling approaches to predict drug response in clinical oncology. *Yonsei Med J*. 2017;58:1-8.
22. Ribba B, Holford NH, Magni P, et al. A review of mixed-effects models of tumor growth and effects of anticancer drug treatment used in population analysis. *CPT Pharmacometrics Syst Pharmacol*. 2014;3:e113.
23. Chan P, Marchand M, Yoshida K, et al. Prediction of overall survival in patients across solid tumors following atezolizumab treatments: A tumour growth inhibition-overall survival

modeling framework. *CPT Pharmacometrics Syst Pharmacol.* 2021;10:1171-1182.

24. Joerger M, vom Pawel J, Kraff S, et al. Open-label, randomized study of individualized, pharmacokinetically (PK)-guided dosing of paclitaxel combined with carboplatin or cisplatin in patients with advanced non-small-cell lung cancer (NSCLC). *Ann Oncol.* 2016;27:1895-1902.

25. Henrich A et al. Semimechanistic bone marrow exhaustion pharmacokinetic/pharmacodynamic model for chemotherapy-induced cumulative neutropenia. *J Pharmacol Exp Ther.* 2017;362:347-358.

26. Ojara FW, Henrich A, Frances N, et al. Time-to-event analysis of paclitaxel-associated peripheral neuropathy in advanced non–small-cell lung cancer highlighting key influential treatment/patient factors. *J Pharmacol Exp Ther.* 2020;375:430-438.

27. Johansson ÅM, Karlsson MO. Multiple imputation of missing covariates in NONMEM and evaluation of the method's sensitivity to η-shrinkage. *AAPS J.* 2013;15:1035-1042.

28. Svensson EM, Svensson RJ, te Brake LHM, et al. The potential for treatment shortening with higher rifampicin doses: relating drug exposure to treatment response in patients with pulmonary tuberculosis. *Clin Infect Dis.* 2018;67:34-41.

29. Wahlby U, Jonsson EN, Karlsson MO. Comparison of stepwise covariate model building strategies in population pharmacokinetic-pharmacodynamic analysis. *AAPS PharmSci.* 2002;4:E27.

30. Mould DR, Upton RN. Basic concepts in population modeling, simulation, and model-based drug development-part 2: introduction to pharmacokinetic modeling methods. *CPT Pharmacometrics Syst Pharmacol.* 2013;2:e38.

31. Bergstrand M, Hooker AC, Wallin JE, Karlsson MO. Prediction-corrected visual predictive checks for diagnosing nonlinear mixed-effects models. *AAPS J.* 2011;13:143-151.

32. R Core Team. *R: A Language and Environment for Statistical Computing.* R Foundation for statistical Computing; 2021. Accessed April 27, 2021. https://www.r-project.org/

33. Lindbom L, Pihlgren P, Jonsson N. Erratum: PsN-toolkit - a collection of computer intensive statistical methods for non-linear mixed effect modeling using NONMEM. *Comput Methods Programs Biomed.* 2005;79:241-257.

34. Keizer RJ, van Benten M, Beijnen JH, Schellens JHM, Huitema ADR. Piraña and PCluster: a modeling environment and cluster infrastructure for NONMEM. *Comput Methods Programs Biomed.* 2011;101:72-79.

35. Merk J, Rolff J, Dorn C, Leschber G, Fichtner I. Chemoresistance in non-small-cell lung cancer: can multidrug resistance markers predict the response of xenograft lung cancer models to chemotherapy? *Eur J Cardiothorac Surg.* 2011;40:29-33.

36. Lara PN Jr, Redman MW, Kelly K, et al. Disease control rate at 8 weeks predicts clinical benefit in advanced non-small-cell lung cancer: results from southwest oncology group randomized trials. *J Clin Oncol.* 2008;26:463-467.

37. He L, Teng Y, Jin B, et al. Initial partial response and stable disease according to RECIST indicate similar survival for chemotherapeutical patients with advanced non-small cell lung cancer. *BMC Cancer.* 2010;10:681.

38. Zecchin C, Gueorguieva I, Enas NH, Friberg LE. Models for change in tumour size, appearance of new lesions and survival probability in patients with advanced epithelial ovarian cancer. *Br J Clin Pharmacol.* 2016;82:717-727.

39. Jain S, Gautam V, Naseem S. Acute-phase proteins: As diagnostic tool. *J Pharm Bioallied Sci.* 2011;3:118-127.

40. Aref H, Refaat S. CRP evaluation in non-small cell lung cancer. *Egypt J Chest Dis Tuberc.* 2014;63:717-722.

41. Scott HR, McMillan DC, Forrest LM, Brown DJF, McArdle CS, Milroy R. The systemic inflammatory response, weight loss, performance status and survival in patients with inoperable non-small cell lung cancer. *Br J Cancer.* 2002;87:264-267.

42. Sproston NR, Ashworth JJ. Role of C-reactive protein at sites of inflammation and infection. *Front Immunol.* 2018;9:754.

43. Shrotriya S, Walsh D, Bennani-Baiti N, Thomas S, Lorton C. C-reactive protein is an important biomarker for prognosis tumor recurrence and treatment response in adult solid tumors: a systematic review. *PLoS One.* 2015;10:e0143080.

44. Holdenrieder S, Nagel D, Stieber P. Estimation of prognosis by circulating biomarkers in patients with non-small cell lung cancer. *Cancer Biomark.* 2009;6:179-190.

45. Gavrilov S, Zhudenkov K, Helmlinger G, Dunyak J, Peskov K, Aksenov S. Longitudinal tumor size and neutrophil-to-lymphocyte ratio are prognostic biomarkers for overall survival in patients with advanced non-small cell lung cancer treated with durvalumab. *CPT Pharmacometrics Syst Pharmacol.* 2021;10:67-74.

46. Grisic AM, Eser A, Huisinga W, Reinisch W, Kloft C. Quantitative relationship between infliximab exposure and inhibition of C-reactive protein synthesis to support inflammatory bowel disease management. *Br J Clin Pharmacol.* 2020;87:2374-2384.

47. Kluwe F, Michelet R, Mueller-Schoell A, et al. Perspectives on model-informed precision dosing in the digital health era: challenges, opportunities, and recommendations. *Clin Pharmacol Ther.* 2021;109:29-36.

48. Klopp-Schulze L, Mueller-Schoell A, Neven P, et al. Integrated data analysis of six clinical studies points toward model-informed precision dosing of tamoxifen. *Front Pharmacol.* 2020;11:283.

49. Cline DJ, Zhang H, Lundell GD, et al. Development and evaluation of a nanoparticle-based immunoassay for determining paclitaxel concentrations on routine clinical analyzers. *Ther Drug Monit.* 2013;35:809-815.

50. Scharnhorst V, Noordzij PG, Lutz A, Graser U, Püntener D, Alquézar-Arbé A. A multicenter evaluation of a point of care CRP test. *Clin Biochem.* 2019;71:38-45.

SUPPORTING INFORMATION

Additional supporting information can be found online in the Supporting Information section at the end of this article.